Optimal Blind Carrier Recovery for MPSK Burst Transmissions

Yan Wang, Erchin Serpedin, and Philippe Ciblat

***Abstract*—This paper introduces and analyzes the asymptotic (large sample) performance of a family of blind feedforward nonlinear least-squares (NLS) estimators for joint estimation of carrier phase, frequency offset, and Doppler rate for burst-mode phase-shift keying transmissions. An optimal or "matched" nonlinear estimator that exhibits the smallest asymptotic variance within the family of envisaged blind NLS estimators is developed. The asymptotic variance of these estimators is established in closed-form expression and shown to approach the Cramèr–Rao lower bound of an unmodulated carrier at medium and high signal-to-noise ratios (SNR). Monomial nonlinear estimators that do not depend on the SNR are also introduced and shown to perform similarly to the SNR-dependent matched nonlinear estimator. Computer simulations are presented to corroborate the theoretical performance analysis.**

***Index Terms*—Burst transmission, carrier phase, Doppler rate, frequency offset, M-ary phase-shift keying (MPSK), synchronization.**

I. INTRODUCTION

BURST transmission of digital data and voice is employed in time-division multiple access (TDMA) and packet demand-assignment multiple access (DAMA) satellite communication and terrestrial mobile cellular radio systems. Conventionally, carrier synchronization of burst transmissions requires a large number of overhead symbols, which results in reduced spectral efficiency and increased transmission delays [7].

Non-data aided (NDA) or blind feedforward carrier synchronization of burst M-ary phase-shift keying (MPSK) transmissions has received much attention in the literature. A generalized form of the maximum-likelihood feedforward (ML FF) algorithm was originally proposed by A. J. Viterbi and A. M. Viterbi as a blind carrier phase estimator with improved performance at low and intermediate signal-to-noise ratios (SNRs) [21], [25]. This carrier phase estimator is referred to as the Viterbi and Viterbi (V&V) algorithm [8], [17], [19, p. 280], and has been used to design blind frequency offset estimators for burst MPSK modulations transmitted through additive white Gaussian noise (AWGN) channels [2]–[5], [9]. Extensions of the V&V carrier estimator for flat Rayleigh and Ricean fading channels were reported in [23] and [10]. The V&V estimator exhibits several desirable features: its good performance at low SNRs translates into improved bit-error probability (BEP) performance in fading channels that tend to be dominated by times when the signal experiences a deep fade (low SNR), and its open-loop operation enables fast reliable acquisitions after deep fades [23]. Reference [8] introduces a different class of blind carrier frequency estimators that assume fractional sampling of the received signal. However, the statistical properties of the resulting estimators are partially analyzed based on certain approximations [8]. A quite general blind nonlinear least-squares (NLS) estimator for the carrier phase, frequency offset, and Doppler rate was proposed in [18]. However, the performance of the NLS-type estimator was not analyzed and exploited to develop carrier recovery algorithms with improved performance [18].

In this paper, a family of blind feedforward joint carrier phase, frequency offset, and Doppler rate NLS estimators for carriers that are fully modulated by MPSK modulations is proposed based on the V&V algorithm. An optimal or "matched" nonlinear estimator that achieves the smallest asymptotic (large sample) variance within the family of blind NLS estimators is also proposed. Monomial nonlinear estimators that do not require knowledge of the SNR are developed and shown to perform similarly to the matched nonlinear estimator. A thorough and rigorous analysis of the statistical properties of the proposed family of NLS carrier synchronizers in AWGN and flat Ricean-fading channels is proposed and exploited to develop estimators with improved performance.

As we shall see, the proposed family of blind NLS estimators presents high convergence rates, provides high accurate estimates for phase, frequency offset, and Doppler rate, and admits low-complexity digital implementations, without being necessary to oversample (or fractionally sample) the received signal faster than the Nyquist rate [8]. The performance of these algorithms coincides with the Cramèr–Rao bound (CRB) of an unmodulated carrier at medium and high SNRs, and is robust to Ricean fading effects and timing errors.

The rest of this paper is organized as follows. In Section II, the discrete-time channel model is described. Section III introduces the family of blind NLS estimators for carrier phase, frequency offset, and Doppler rate. The asymptotic performance of these estimators is established in closed-form expression and

Paper approved by R. Reggiannini, the Editor for Synchronization and Wireless Applications of the IEEE Communications Society. Manuscript received October 31, 2001; revised October 9, 2002 and February 10, 2003. This work was supported by the National Science Foundation under Award CCR-0092901. This paper was presented in part at the 2002 International Conference on Acoustics, Speech, and Signal Processing, Orlando, FL, May 2002, and in part at the 2002 IEEE International Conference on Communications, New York, NY, May 2002.

Y. Wang and E. Serpedin are with the Department of Electrical Engineering, Texas A&M University, College Station, TX 77843-3128 USA (e-mail: wangyan@ee.tamu.edu; serpedin@ee.tamu.edu).

P. Ciblat is with Ecole Nationale Supérieure des Télécommunications, Departement Communications et Electronique, F-75013 Paris, France (e-mail: philippe.ciblat@enst.fr).

Digital Object Identifier 10.1109/TCOMM.2003.816979

exploited to develop optimal or "matched" nonlinear estimators that exhibit minimum variance. In Section IV, the optimal nonlinearity is approximated by a class of monomial transformations and the asymptotic performance of resulting estimators is established. The results of Section IV are extended to flat Ricean-fading channels in Section V. A high-order ambiguity function (HAF)-based estimator is briefly introduced in Section VI to decrease the computational load of the NLS estimators. In Section VII, simulation results are conducted to confirm our theoretical analysis. Finally, in Section VIII, conclusions are drawn, and detailed mathematical derivations of the proposed performance analyzes are reported in the Appendixes.

II. Problem Formulation

Consider the baseband representation of an MPSK-modulated signal transmitted through an AWGN channel. Assume that filtering is evenly split between transmitter and receiver so that the overall channel satisfies the first Nyquist condition. Filtering the received waveform through a matched filter and sampling at the right time instants yields

$$\begin{aligned} x(n) &= w(n)e^{j\phi(n)} + v(n), \qquad n = 0,\ldots,N-1 \\ \phi(n) &= \theta + 2\pi F_e T n + \eta T^2 n^2 \end{aligned} \tag{1}$$

where $\{w(n)\}$ is the sequence of zero-mean unit variance[1] $(\sigma_w^2 := \mathrm{E}\{|w(n)|^2\} = 1)$ independently and identically distributed (i.i.d.) MPSK symbols, θ, F_e, and η stand for carrier phase, frequency offset, and Doppler rate, respectively, T denotes the symbol period, and $\{v(n)\}$ is a zero-mean circular white Gaussian noise process independent of $w(n)$ and with variance $\sigma_v^2 := \mathrm{E}\{|v(n)|^2\}$. The SNR is defined as $\mathrm{SNR} := 10\log_{10}(\sigma_w^2/\sigma_v^2)$.

As depicted by (1), the problem that we pose is to estimate the unknown phase parameters (θ, F_e, and η) of a random amplitude chirp signal $\exp(j\phi(n))$ embedded in unknown additive noise, assuming knowledge of the received samples $\{x(n)\}_{n=0}^{N-1}$. The solution that we pursue consists of evaluating first certain moments of the output that will remove the unwanted multiplicative effects introduced by the MPSK modulated sequence $w(n)$. It turns out that the resulting problem reduces to the standard problem of estimating the phase parameters of a constant amplitude chirp signal embedded in additive noise, for which standard NLS-type estimators can be developed and their statistical properties analyzed in a rigorous manner.

III. Nonlinear Carrier Synchronizer

Consider the polar representation of $x(n)$

$$x(n) = \rho(n)e^{j\varphi(n)} \tag{2}$$

and define the process $y(n)$ via the nonlinear transformation

$$y(n) := F(\rho(n))\, e^{jM\varphi(n)} \tag{3}$$

where $F(\cdot)$ is a real-valued nonlinear function.

Conditioned on the MPSK symbol $w(n)$, $x(n)$ is normally distributed with the probability density function (pdf) $f(x(n)|w(n) = \exp(j2\pi m/M),\ 0 \le m \le M-1) \sim \mathcal{N}(w(n)\exp(j\phi(n)), \sigma_v^2)$. Due to (2), it follows that

$$\begin{aligned} f\left(\rho(n), \varphi(n) | w(n) = \exp\left(\frac{j2\pi m}{M}\right)\right) \\ = \frac{\rho(n)}{\pi\sigma_v^2} e^{-\frac{\left(\rho^2(n)+1\right)}{\sigma_v^2}} e^{2\rho(n)\frac{\cos\left[\varphi(n) - \frac{2\pi m}{M} - \phi(n)\right]}{\sigma_v^2}}. \end{aligned} \tag{4}$$

Based on (4), the joint pdf of $\rho(n)$ and $\varphi(n)$, and the marginal pdf of $\rho(n)$ take the expressions

$$\begin{aligned} f(\rho(n),\varphi(n)) &= \frac{1}{M}\sum_{m=0}^{M-1} f\left(\rho(n),\varphi(n)|w(n) = \exp\left(\frac{j2\pi m}{M}\right)\right) \\ &= \frac{1}{M}\sum_{m=0}^{M-1} \frac{\rho(n)}{\pi\sigma_v^2} e^{-\frac{\rho^2(n)+1}{\sigma_v^2}} \\ &\quad \times e^{\frac{2\rho(n)}{\sigma_v^2}\cos\left[\varphi(n) - \frac{2\pi m}{M} - \phi(n)\right]} \end{aligned} \tag{5}$$

$$\begin{aligned} f(\rho(n)) &= \int_{-\pi}^{\pi} f(\rho(n),\varphi(n))\, \mathrm{d}\varphi(n) \\ &= \frac{2\rho(n)}{\sigma_v^2} e^{-\frac{\left(\rho^2(n)+1\right)}{\sigma_v^2}} I_0\left(\frac{2\rho(n)}{\sigma_v^2}\right) \end{aligned} \tag{6}$$

respectively, where $I_0(\cdot)$ stands for the zero-order modified Bessel function of the first kind [1, eq. (9.6.16)]. Moreover, it is not difficult to find that the joint pdf of the random variables (RVs) $\rho(n_1)$, $\varphi(n_1)$, $\rho(n_2)$, $\varphi(n_2)$ satisfies the following relation:

$$\begin{aligned} f(\rho(n_1),\varphi(n_1),\rho(n_2),\varphi(n_2)) &= f(\rho(n_1),\varphi(n_1)) \\ &\cdot f(\rho(n_2),\varphi(n_2)), \qquad \text{for } n_1 \ne n_2. \end{aligned} \tag{7}$$

Exploiting (5) and (6), some calculations, whose details are provided in Appendix I, lead to the following relations:

$$\mathrm{E}\{y(n)\} = \mathrm{E}\left\{F(\rho(n))\, e^{jM\varphi(n)}\right\} = \mathcal{C}e^{jM\phi(n)} \tag{8}$$

$$\mathcal{C} := |\mathrm{E}\{y(n)\}| = \mathrm{E}\left\{F(\rho(n))\frac{I_M\left(\frac{2\rho(n)}{\sigma_v^2}\right)}{I_0\left(\frac{2\rho(n)}{\sigma_v^2}\right)}\right\} \tag{9}$$

where $I_M(\cdot)$ denotes the Mth-order modified Bessel function of the first kind [1, eq. (9.6.19)], the expectation in (9) is with respect to (w.r.t.) the marginal distribution of $\rho(n)$ (6), and the resulting amplitude $\mathcal{C}$ is a real-valued constant which does not depend on n. Since $w(n)$ and $v(n)$ are i.i.d. and mutually independent, from (7), it follows that $u(n) := y(n) - \mathrm{E}\{y(n)\}$ is i.i.d., too. Consequently

$$y(n) = \mathcal{C}e^{jM\phi(n)} + u(n), \qquad n = 0, 1, \ldots, N-1 \tag{10}$$

and $y(n)$ can be viewed as a constant amplitude chirp signal $\exp(jM\phi(n))$ embedded in white noise. Note that, in general, the white noise process $u(n)$ is not circular.

Let $\boldsymbol{\omega} := [\mathcal{C}\ \omega_0\ \omega_1\ \omega_2]^T = [\mathcal{C}\ M\theta\ 2\pi MF_eT\ M\eta T^2]^T$, and introduce the following NLS estimator (c.f. [13], [18]):

$$\hat{\boldsymbol{\omega}} = \arg\min_{\bar{\boldsymbol{\omega}}} J(\bar{\boldsymbol{\omega}}) \tag{11}$$

$$J(\bar{\boldsymbol{\omega}}) = \frac{1}{2}\sum_{n=0}^{N-1}\left|y(n) - \bar{\mathcal{C}}e^{j\sum_{l=0}^{2}\bar{\omega}_l n^l}\right|^2. \tag{12}$$

[1]Notation ":=" stands for "is defined as".

By equating to zero the gradient of $J(\bar{\boldsymbol{\omega}})$, some simple algebra calculations lead to the following expressions for the NLS estimates of ω_l, $l=0, 1, 2$ [13]:

$$(\hat{\omega}_1, \hat{\omega}_2) = \arg\max_{\bar{\omega}_1, \bar{\omega}_2} \frac{1}{N} \left| \sum_{n=0}^{N-1} y(n) e^{-j\sum_{l=1}^{2} \bar{\omega}_l n^l} \right|^2$$
$$\hat{\omega}_0 = \text{angle} \left\{ \sum_{n=0}^{N-1} y(n) e^{-j\sum_{l=1}^{2} \hat{\omega}_l n^l} \right\}. \quad (13)$$

It is well known that estimator (11) is asymptotically unbiased and consistent, and also almost asymptotically efficient at high SNR [6], [12], [13].

Following a procedure similar to the one presented in [13], one can derive the asymptotic variances of estimates $\hat{\omega}_l$, $l=0$, 1, 2. These calculations are established in Appendix II and are summarized in the following theorem.

Theorem 1: The asymptotic variances of the NLS estimates $\hat{\omega}_l$, $l=0, 1, 2$ in (11)–(13) are given by

$$\text{avar}(\hat{\omega}_l) = \frac{\mathcal{B}-\mathcal{D}}{\mathcal{C}^2} \cdot \frac{1}{2N^{2l+1}} \cdot \frac{1}{2l+1} \cdot \left[\frac{(l+3)!}{(l!)^2 (2-l)!} \right]^2 \quad (14)$$
$$\mathcal{B} := \text{E}\left\{ |y(n)|^2 \right\} = \text{E}\left\{ F^2(\rho(n)) \right\} \quad (15)$$
$$\mathcal{D} := \left| \text{E}\left\{ y^2(n) \right\} \right| = \left| \text{E}\left\{ F^2(\rho(n)) e^{j2M\varphi(n)} \right\} \right|$$
$$= \text{E}\left\{ F^2(\rho(n)) \frac{I_{2M}\left(\frac{2\rho(n)}{\sigma_v^2}\right)}{I_0\left(\frac{2\rho(n)}{\sigma_v^2}\right)} \right\} \quad (16)$$

and $\mathcal{C}$ is defined in (9).

Some remarks are now in order.

Remark 1: From (14)–(16), one can observe that the asymptotic variances of $\hat{\omega}_l$, $l=0, 1, 2$ are independent of the unknown phase parameters θ, F_e, and η.

Remark 2: It is of interest to compare the asymptotic variances (14) with the CRB. In [11] and [12], the CRB is derived for the case when the random amplitude $w(n)$ of model (1) is a stationary Gaussian process. In [13], the CRB is obtained by assuming that the additive noise $u(n)$ of model (10) is colored Gaussian and circularly symmetric. Note that in this paper, both models (1) and (10) do not satisfy these assumptions. Therefore, in this paper, we adopt the CRB for an unmodulated carrier wave (UCRB), i.e., $M=1$ (c.f. [25]), which is a special case of the CRB presented in [11]–[13]

$$\text{UCRB}(\hat{\omega}_l) = \frac{\sigma_v^2}{2N^{2l+1}} \cdot \frac{1}{2l+1} \cdot \left[\frac{(l+3)!}{(l!)^2 (2-l)!} \right]^2. \quad (17)$$

Based on (14), one can observe that the asymptotic variances $\text{avar}(\hat{\omega}_l)$ of the NLS estimates $\hat{\omega}_l$, $l=0, 1, 2$, decay at the same rate as the UCRB, i.e., $\text{O}(1/N^{2l+1})$.

Remark 3: Estimator (13) involves a two-dimensional (2-D) maximization problem which could be too intensive if a good initial estimate cannot be provided. In this paper, the initial values of F_e and η are obtained by the so-called HAF approach, which has become a "standard" tool for analyzing constant amplitude chirp signals since it provides a computationally efficient yet statistically accurate estimator [6]. We will briefly introduce the HAF-based estimator in Section VI.

Remark 4: The estimates of phase parameters θ, F_e, and η present M-fold ambiguity, which can be counteracted by applying differential encoding [18] or unique word decoding method [23]. The estimation range due to the ambiguity, e.g., for F_e, is $|F_e| < 1/(2MT)$.

Next, we determine the optimal or "matched" nonlinearity $F(\cdot)$ which minimizes the asymptotic variance $\text{avar}(\hat{\omega}_l)$ (14). Since in (14), only the terms $\mathcal{B}$, $\mathcal{C}$, and $\mathcal{D}$ depend on $F(\cdot)$, finding an optimal $F(\cdot)$ resorts to solving the optimization problem

$$F_{\min}(\rho(n)) = \arg\min_{F(\cdot)} \frac{\mathcal{B}-\mathcal{D}}{\mathcal{C}^2}.$$

Using (9), (15), and (16), we obtain

$$\frac{\mathcal{B}-\mathcal{D}}{\mathcal{C}^2} = \frac{\text{E}\left\{ F^2(\rho(n)) \left(1 - \frac{I_{2M}\left(\frac{2\rho(n)}{\sigma_v^2}\right)}{I_0\left(\frac{2\rho(n)}{\sigma_v^2}\right)} \right) \right\}}{\text{E}\left\{ F(\rho(n)) \frac{I_M\left(\frac{2\rho(n)}{\sigma_v^2}\right)}{I_0\left(\frac{2\rho(n)}{\sigma_v^2}\right)} \right\}}.$$

Using Cauchy–Schwarz' inequality, the optimum nonlinearity $F_{\min}$ is given by the following theorem.

Theorem 2: The optimal or "matched" nonlinearity $F_{\min}(\cdot)$ that minimizes the asymptotic variances of the proposed family of NLS estimators (11) is given by

$$F_{\min}(\rho(n)) = \lambda \frac{I_M\left(\frac{2\rho(n)}{\sigma_v^2}\right)}{I_0\left(\frac{2\rho(n)}{\sigma_v^2}\right) - I_{2M}\left(\frac{2\rho(n)}{\sigma_v^2}\right)} \quad (18)$$

where λ is an arbitrary nonzero constant. Plugging (18) back into (9), (15), and (16), and substituting these values into (14), the minimal asymptotic variances of $\hat{\omega}_l$, $l=0, 1, 2$ can be expressed as

$$\text{avar}_{\min}(\hat{\omega}_l) = \frac{1}{2N^{2l+1}} \cdot \frac{1}{2l+1} \cdot \left[\frac{(l+3)!}{(l!)^2 (2-l)!} \right]^2 \cdot \frac{1}{\text{E}\left\{ \frac{I_M^2\left(\frac{2\rho(n)}{\sigma_v^2}\right)}{I_0^2\left(\frac{2\rho(n)}{\sigma_v^2}\right) - I_0\left(\frac{2\rho(n)}{\sigma_v^2}\right) I_{2M}\left(\frac{2\rho(n)}{\sigma_v^2}\right)} \right\}}. \quad (19)$$

IV. Monomial Nonlinearity Estimators

As can be observed from (18), $F_{\min}(\rho(n))$ is a function that depends on the SNR. This is not a restrictive requirement since blind SNR estimators that exhibit good performance can be used [22]. However, if the SNR estimation step is not desirable, we show next that there exist optimal monomial approximations $\rho^k(n)$, $k=0,\ldots,M$, of the matched nonlinearity $F_{\min}(\rho(n))$ that exhibit almost the same asymptotic variance as (19) and their implementation does not require knowledge of the SNR.

Exploiting the asymptotic formula [1, eq. (9.7.1)] in (18), it turns out that at high SNRs $(\text{SNR} \to \infty)$ the optimal monomial is $G_h(\rho(n)) = \rho(n)$. Similarly, based on [1, eq. (9.6.7)], it turns out that at low SNRs $(\text{SNR} \to -\infty)$, the optimal monomial is $G_l(\rho(n)) = \rho^M(n)$. These results parallel the derivations reported in [21] and do not depend on the value of the frequency shift or Doppler rate. In order to obtain a better understanding, next we establish the asymptotic performance of the monomial NLS estimators.

Define the class of processes $y_k(n)$ by means of the monomial transformations

$$y_k(n) = \rho^k(n)e^{jM\varphi(n)}, \quad k = 0, 1, \ldots, M \tag{20}$$

and the zero-mean processes $u_k(n) := y_k(n) - \mathrm{E}\{y_k(n)\}$, $k = 0, \ldots, M$. As before, it turns out that $\mathrm{E}\{y_k(n)\}$ is a constant amplitude chirp signal, and hence, $y_k(n) = \mathrm{E}\{y_k(n)\} + u_k(n)$ can be interpreted as a constant amplitude chirp signal embedded in white noise. As a special case of (11), we introduce the following class of monomial NLS estimators:

$$\hat{\boldsymbol{\omega}}^{(k)} = \arg\min_{\bar{\boldsymbol{\omega}}^{(k)}} \frac{1}{2}\sum_{n=0}^{N-1}\left|y_k(n) - \bar{\mathcal{C}}^{(k)}e^{j\sum_{l=0}^{2}\bar{\omega}_l^{(k)}n^l}\right|^2 \tag{21}$$

whose asymptotic variances for $\hat{\omega}_l^{(k)}$, $l =$0, 1, 2 are provided by the following theorem.

Theorem 3: The asymptotic variances of the NLS estimates $\hat{\omega}_l^{(k)}$, $l =$0, 1, 2 in (21), are given by

$$\begin{aligned}\operatorname{avar}\left(\hat{\omega}_l^{(k)}\right) &= \frac{\mathcal{B}_k - \mathcal{D}_k}{\mathcal{C}_k^2}\cdot\frac{1}{2N^{2l+1}}\cdot\frac{1}{2l+1}\cdot\left[\frac{(l+3)!}{(l!)^2(2-l)!}\right]^2\\ \mathcal{B}_k &:= \mathrm{E}\left\{|y_k(n)|^2\right\} = \mathrm{E}\left\{\rho^{2k}(n)\right\}\\ \mathcal{C}_k &:= |\mathrm{E}\{y_k(n)\}| = \left|\mathrm{E}\left\{\rho^k(n)e^{jM\varphi(n)}\right\}\right|\\ \mathcal{D}_k &:= \left|\mathrm{E}\left\{y_k^2(n)\right\}\right| = \left|\mathrm{E}\left\{\rho^{2k}(n)e^{j2M\varphi(n)}\right\}\right|. \end{aligned}\tag{22}$$

Exploiting (6) and [15, eq. (6.643.4)], the following relation was derived in [25, (A17)]:

$$\mathcal{B}_k = \sum_{q=0}^{k}\binom{k}{q}^2\sigma_v^{2q}\cdot q!. \tag{23}$$

Using (5), we can obtain that

$$\begin{aligned}\mathrm{E}\{y_k(n)\} &= \int_0^\infty\int_{-\pi}^{\pi}\rho^k(n)e^{jM\varphi(n)}f(\rho(n),\varphi(n))\,\mathrm{d}\varphi(n)\mathrm{d}\rho(n)\\ &= \frac{1}{M}\sum_{m=0}^{M-1}\int_0^\infty\frac{\rho^{k+1}(n)}{\pi\sigma_v^2}e^{-\frac{\rho^2(n)+1}{\sigma_v^2}}\int_{-\pi}^{\pi}e^{jM\varphi(n)}\\ &\quad\times e^{\frac{2\rho(n)}{\sigma_v^2}\cos\left[\varphi(n)-\frac{2\pi m}{M}-\phi(n)\right]}\mathrm{d}\varphi(n)\mathrm{d}\rho(n)\\ &= \frac{1}{\alpha^k}e^{jM\phi(n)}e^{-\frac{\gamma}{2}}\int_0^\infty\zeta^{k+1}e^{-\frac{\zeta^2}{2}}I_M(\alpha\zeta)\mathrm{d}\zeta\end{aligned}\tag{24}$$

where $\alpha := \sqrt{2}/\sigma_v$, $\gamma := \alpha^2$, and $\zeta := \alpha\rho(n)$. Based on [15, eq. (6.643.2)] and [1, eq. (13.1.32)], $\mathcal{C}_k$ can be expressed in terms of the confluent hypergeometric function $\Phi(\cdot,\cdot,\cdot)$ for $k = 0, 1, \ldots, M$

$$\mathcal{C}_k = \frac{\Gamma\left(\frac{k+M}{2}+1\right)e^{-\frac{\gamma}{2}}}{\Gamma(M+1)\sigma_v^{M-k}}\Phi\left(\frac{k+M}{2}+1,\ M+1,\ \frac{\gamma}{2}\right). \tag{25}$$

Similarly

$$\mathcal{D}_k = \frac{\Gamma(k+M+1)e^{-\frac{\gamma}{2}}}{\Gamma(2M+1)\sigma_v^{2M-2k}}\Phi\left(k+M+1,\ 2M+1,\ \frac{\gamma}{2}\right). \tag{26}$$

It should be pointed out that when k is even (M is usually a power of two), following a similar approach to that presented in [25] or the formula [1, eq. (13.5.1)], one can obtain a slightly more compact expression for the confluent hypergeometric function in (25)

$$\begin{aligned}\mathcal{C}_k &= \frac{1}{\gamma^t}\left[\gamma^t\sum_{p=0}^{s+t}p!\binom{s+t}{p}\binom{s-t+p-1}{p}\right.\\ &\quad\times\left(\frac{-2}{\gamma}\right)^p + (-1)^{s+t+1}2^te^{-\frac{\gamma}{2}}\left(\frac{2}{\gamma}\right)^{t+1}\\ &\quad\left.\times\sum_{p=0}^{s-t-1}\binom{s+t+p}{p}\cdot\frac{(s+t)!}{(s-t-p-1)!}\left(\frac{2}{\gamma}\right)^p\right]\\ &\quad\text{if } k = 0, 2, \ldots, M-2\\ \mathcal{C}_k &= 1, \quad \text{if } k = M\end{aligned}$$

where $s := M/2$ and $t := k/2$. Similarly

$$\begin{aligned}\mathcal{D}_k &= \frac{1}{\gamma^k}\left[\gamma^k\sum_{p=0}^{M+k}p!\binom{M+k}{p}\binom{M-k+p-1}{p}\right.\\ &\quad\times\left(\frac{-2}{\gamma}\right)^p + (-1)^{M+k+1}2^ke^{-\frac{\gamma}{2}}\left(\frac{2}{\gamma}\right)^{k+1}\\ &\quad\left.\cdot\sum_{p=0}^{M-k-1}\binom{M+k+p}{p}\cdot\frac{(M+k)!}{(M-k-p-1)!}\left(\frac{2}{\gamma}\right)^p\right],\\ &\quad\text{if } k = 0, 1, \ldots, M-1\\ \mathcal{D}_k &= 1, \quad \text{if } k = M.\end{aligned}\tag{27}$$

Plugging (23), (25), and (26) back into (22), closed-form expressions for the asymptotic variances $\operatorname{avar}(\hat{\omega}_l^{(k)})$ for $k = 0, 1, \ldots, M$, and $l =$0, 1, 2 are obtained.

Note that at very high SNR ($1/\sigma_v^2 \to \infty$), using [1, eq. (13.1.4)], some calculations show that

$$\lim_{\mathrm{SNR}\to\infty}\mathcal{C}_k = 1 \tag{28}$$

for any $k = 0, 1, \ldots, M$. Hence, based on (22), (23), (27), and (28), we obtain

$$\operatorname{avar}\left(\hat{\omega}_l^{(k)}\right) \propto \frac{M^2}{\mathrm{SNR}}\cdot\frac{1}{N^{2l+1}}$$

which does not depend on the estimator order k, i.e., it turns out that at very high SNRs, the performance of estimators (21) for different nonlinearity orders k is asymptotically the same.

We close this section with the following remark.

Remark 5: Assume that $\eta = 0$, i.e., the received signal is affected only by phase offset and frequency offset. Then, the estimator (21) reduces to

$$\begin{aligned}\hat{f}_e^{(k)} &= \frac{1}{M}\arg\max_{|\bar{f}_0|<\frac{1}{2}}\frac{1}{N}\left|\sum_{n=0}^{N-1}y_k(n)e^{-j2\pi\bar{f}_0n}\right|\\ \hat{\theta}^{(k)} &= \frac{1}{M}\text{angle}\left\{\sum_{n=0}^{N-1}y_k(n)e^{-j2\pi M\hat{f}_e^{(k)}n}\right\}\end{aligned}\tag{29}$$

with $f_e := F_eT$. Based on (29), the frequency offset estimator can be implemented efficiently by means of the fast Fourier transform (FFT) algorithm applied on the sequence $y_k(n)$, which is generally zero-padded with a sufficiently large number of zeros to achieve the precision provided by the asymptotic CRB ($\mathrm{O}(1/N^3)$). The following corollary is obtained directly from *Theorem 3*.

Corollary 1: The asymptotic variance of the class of NLS estimators (29) for f_e is given by

$$\text{avar}\left(\hat{f}_e^{(k)}\right) = \frac{6(\mathcal{B}_k - \mathcal{D}_k)}{4\pi^2 M^2 \mathcal{C}_k^2 N^3} \tag{30}$$

where $\mathcal{B}_k$, $\mathcal{C}_k$, and $\mathcal{D}_k$ are defined in *Theorem 3*.

V. Extension to Flat Ricean-Fading Channels

In the foregoing discussion, we assumed AWGN channels. In this section, we will see that the NLS estimators (11) remain asymptotically unbiased and consistent in the presence of flat Ricean-fading channels. To simplify our derivation, we will only concentrate on the extension of the frequency offset estimators (29).

Assuming a flat Ricean-fading channel model, the input-output relationship of the channel can be expressed as

$$x(n) = \mu(n)w(n)e^{j2\pi F_e T n} + v(n), \quad n = 0,\ldots,N-1 \tag{31}$$

where $\mu(n) = \rho_\mu(n)\exp(j\varphi_\mu(n))$ is the fading process with nonzero mean $\text{E}\{\mu(n)\} := \rho_1 \exp(j\varphi_1)$ and variance $\sigma_\mu^2 := \text{E}\{|\mu(n) - \text{E}\{\mu(n)\}|^2\}$. Using the Jakes model, the second-order correlations of the fading are given by $\text{E}\{[\mu(n) - \text{E}\{\mu(n)\}]^* \cdot [\mu(n+\tau) - \text{E}\{\mu(n+\tau)\}]\} = \sigma_\mu^2 J_0(2\pi f_d \tau)$, where $J_0(.)$ denotes the zero-order Bessel function of the first kind, and f_d stands for the normalized Doppler spread. The joint pdf of $\rho_\mu(n)$ and $\varphi_\mu(n)$, and the marginal pdf of $\rho_\mu(n)$ are given by

$$f(\rho_\mu(n), \varphi_\mu(n)) = \frac{\rho_\mu(n)}{\pi\sigma_\mu^2} e^{-\frac{\rho_\mu^2(n) + \rho_1^2 - 2\rho_\mu(n)\rho_1 \cos(\varphi_\mu(n) - \varphi_1)}{\sigma_\mu^2}} \tag{32}$$

$$f(\rho_\mu(n)) = \frac{2\rho_\mu(n)}{\sigma_\mu^2} e^{-\frac{\rho_\mu^2(n) + \rho_1^2}{\sigma_\mu^2}} I_0\left(\frac{2\rho_\mu(n)\rho_1}{\sigma_\mu^2}\right). \tag{33}$$

Conditioned on the fading process $\mu(n)$ and the input symbol $w(n)$, the joint pdf of $\rho(n)$ and $\varphi(n)$ takes the form

$$\begin{aligned} f&\left(\rho(n), \varphi(n) | w(n) = \exp\left(\frac{j2\pi l}{M}\right), \rho_\mu(n), \varphi_\mu(n)\right) \\ &= \frac{\rho(n)}{\pi\sigma_v^2} e^{-\frac{\left(\rho^2(n) + \rho_\mu^2(n)\right)}{\sigma_v^2}} \\ &\quad \cdot e^{2\rho(n)\rho_\mu(n)\frac{\cos\left[\varphi(n) - \varphi_\mu(n) - \frac{2\pi(l + M f_e n)}{M}\right]}{\sigma_v^2}}. \end{aligned} \tag{34}$$

Using (31)through (34), in a similar way to that presented in the former sections, some straightforward but lengthy calculations lead to

$$\begin{aligned} \text{E}\{y_k(n)\} &= \mathcal{C}_k e^{jM\varphi_1} e^{j2\pi M f_e n}, \qquad k = 0, 1, \ldots, M \\ \mathcal{C}_k &:= \frac{\Gamma\left(\frac{k+M}{2} + 1\right) e^{-\frac{\gamma_1}{2}} \rho_1^M}{\Gamma(M+1)\sigma_1^{M-k}} \Phi\left(\frac{k+M}{2} + 1, M+1, \frac{\gamma_1}{2}\right) \end{aligned}$$

with $\sigma_1^2 := \sigma_\mu^2 + \sigma_v^2$ and $\gamma_1 := 2\rho_1^2/\sigma_1^2$. Hence, $y_k(n)$ can still be viewed as a constant amplitude harmonic embedded in additive noise $u_k(n) := y_k(n) - \text{E}\{y_k(n)\}$, and the unbiasedness and consistency of estimators (29) hold true in the presence of flat Ricean-fading channels. However, we should note that due to the fading effect, $u_k(n)$ is not white any more, but a zero-mean colored process. Establishing the asymptotic variance of estimators (29) in flat Ricean-fading effects for any k is generally, if not impossible, at least very complicated for $k = 0,\ldots,M-1$. In the special case $k = M$, $u_M(n)$ is a circular noise process, whose autocorrelation and spectral density are given by $r_{u_M}(\tau) := \text{E}\{u_M^*(n)u_M(n+\tau)\}$ and $S_{u_M}(f) := \sum_\tau r_{u_M}(\tau)\exp(-j2\pi f\tau)$, respectively. Therefore, the asymptotic variance of (29) is now given by [24]

$$\text{avar}\left(\hat{f}_e^{(M)}\right) = \frac{6 S_{u_M}(M f_e)}{4\pi^2 M^2 \mathcal{C}_M^2 N^3}. \tag{35}$$

The calculation of the power spectral density $S_{u_M}(\cdot)$ is tractable and is briefly detailed next. Define the following variables:

$$\begin{aligned} c_v^{(k)} &:= \text{E}\left\{|v(n)|^{2k}\right\} = k! \cdot \sigma_v^{2k} \\ c_\mu^{(k)} &:= \text{E}\left\{|\mu(n) - \text{E}\{\mu(n)\}|^{2k}\right\} = k! \cdot \sigma_\mu^{2k} \\ r_\mu^{(k)} &:= \text{E}\left\{|\mu(n)|^{2k}\right\} = \rho_1^{2k} + \sum_{l=1}^{k} \binom{k}{l}^2 \rho_1^{2k-2l} c_\mu^{(l)}. \end{aligned}$$

Some direct but lengthy calculations lead to the following expression:

$$\begin{aligned} S_{u_M}(M f_e) = \sum_\tau \sum_{k=1}^{M} \binom{M}{k}^2 \rho_1^{2M-2k} \\ \times c_\mu^{(k)} J_0^k(2\pi f_d \tau) + \sum_{k=1}^{M} \binom{M}{k}^2 c_v^{(k)} r_\mu^{(M-k)}. \end{aligned} \tag{36}$$

Plugging (36) back into (35), a closed-form expression of the asymptotic variance $\text{avar}(\hat{f}_e^{(M)})$ in the presence of flat Ricean-fading effects is obtained.

VI. HAF-Based Estimator

As mentioned in Section III, a HAF-based estimator is a simple and computational efficient approach to provide the initial estimates of NLS estimator (13), and combines the use of the HAF in order to reduce the order of the polynomial phase $\phi(n)$ and that of the NLS approach in order to estimate the parameters of an exponential signal embedded in noise [6].

First, let us rewrite (10) as

$$y(n) = \mathcal{C} e^{j(M\theta + 2\pi M F_e T n + M\eta T^2 n^2)} + u(n)$$

and define the following process:

$$\begin{aligned} y_2(n;\tau) &:= y^*(n) y(n+\tau) \\ &= \mathcal{C}^2 e^{j(2\pi M F_e T\tau + M\eta T^2\tau^2)} e^{j2M\eta T^2 n\tau} + u'(n) \end{aligned} \tag{37}$$

where $\tau > 0$ and $u'(n)$ is a zero-mean noise composed of noise $\times$ signal and noise $\times$ noise terms. For a fixed τ, $y_2(n;\tau)$ is an exponential signal with constant amplitude $\mathcal{C}^2 \exp(j(2\pi M F_e T\tau + M\eta T^2\tau^2))$ embedded in additive noise $u'(n)$. Hence, it is natural to use an NLS estimator to obtain an estimate of η as follows:

$$\hat{\eta} = \frac{1}{2MT^2\tau} \arg\max_{|\bar{\omega}|<\pi} \frac{1}{N} \left|\sum_{n=0}^{N-1} y_2(n;\tau) e^{-j\bar{\omega}n}\right|. \tag{38}$$

Once $\hat{\eta}$ is available, demodulate $y(n)$ to obtain

$$z(n) := y(n) \cdot e^{-jM\hat{\eta}T^2 n^2} \simeq \mathcal{C} e^{j(M\theta + 2\pi M F_e T n)} + u''(n)$$

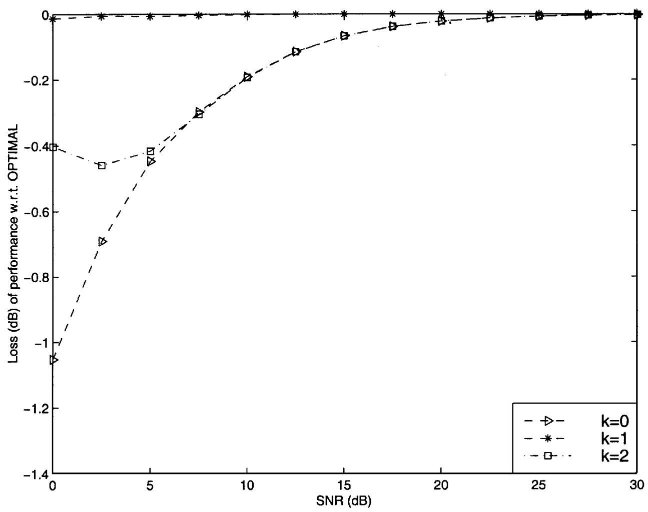

Fig. 1. Theoretical degradation of $\hat{\omega}_l^{(k)}$ w.r.t. the matched nonlinear estimator versus SNR (BPSK constellation, $N = 50$).

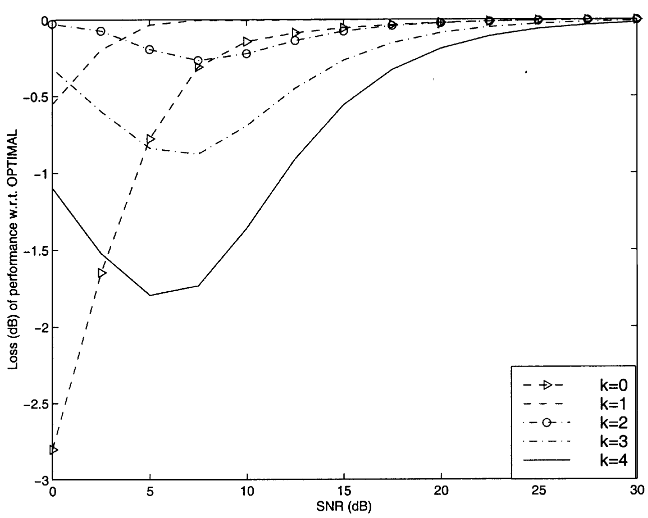

Fig. 2. Theoretical degradation of $\hat{\omega}_l^{(k)}$ w.r.t. the matched nonlinear estimator versus SNR (QPSK constellation, $N = 50$).

where $u''(n)$ combines the estimation errors in $\hat{\eta}$ and the effect of additive noise [6]. Similarly, F_e can be obtained as

$$\hat{F}_e = \frac{1}{MT} \arg \max_{|\bar{f}_0| < \frac{1}{2}} \frac{1}{N} \left| \sum_{n=0}^{N-1} z(n) e^{-j2\pi \bar{f}_0 n} \right|. \quad (39)$$

The HAF-based estimators (38) and (39) can decrease computational complexity and provide good initial values for NLS estimator (13). Examining its performance is beyond the scope of this paper. We refer the reader to [6] for the detailed performance analysis of HAF-based estimator.

VII. Simulation Experiments

In this section, we study thoroughly the performance of estimators (11), (21), and (29) using computer simulations. The experimental mean-square error (MSE) results of these estimators will be compared with the theoretical asymptotic bounds and the CRB-like bounds. The experimental results are obtained by performing a number of 200 Monte Carlo trials, the additive noise is generated as zero-mean Gaussian white noise with variance σ_v^2, and unless otherwise noted, all the simulations are performed assuming the carrier phase $\theta = 0.1$, frequency offset $F_e T = 0.011$, and Doppler rate $\eta T^2 = 0.03$.

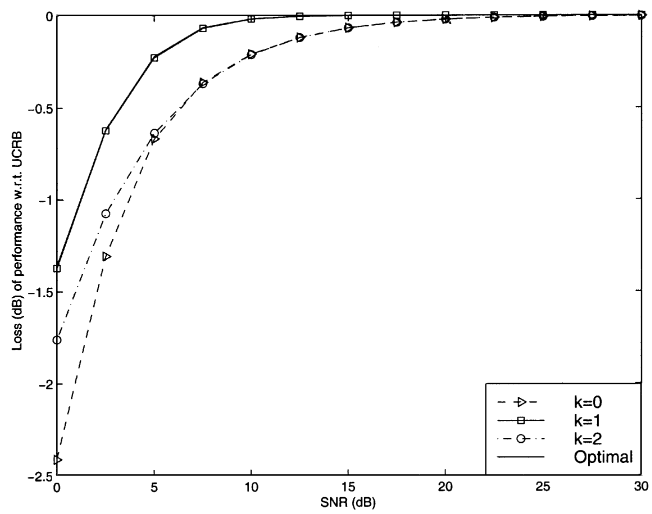

Fig. 3. Performance loss w.r.t. the UCRB versus SNR (BPSK modulation, $N = 50$).

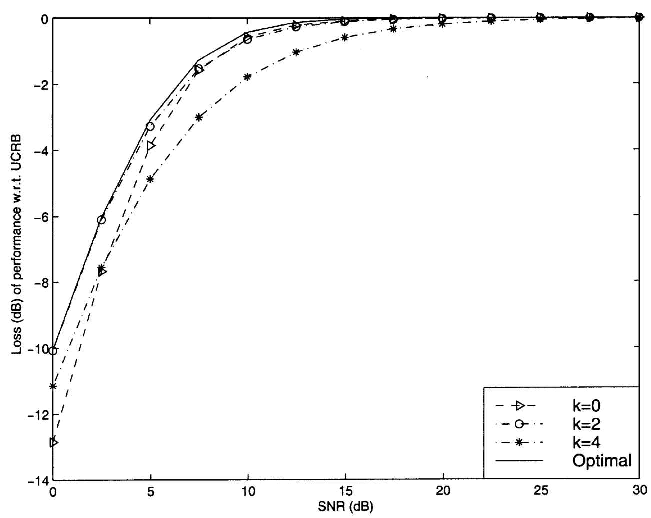

Fig. 4. Performance loss w.r.t. the UCRB versus SNR (QPSK modulation, $N = 50$).

Experiment 1-Performance Loss of Estimators (20), (21) w.r.t. the Matched Estimator (18), (11): Figs. 1 and 2 plot the loss in performance of estimators (20) and (21) w.r.t. the optimal nonlinearity estimator (18), (11) $(-10\log_{10}[\text{avar}(\hat{\omega})_l^{(k)})/\text{avar}_{\min}(\hat{\omega}_l)])$ in the case of a binary phase-shift keying (BPSK) modulation $(M = 2)$ and quaternary phase-shift keying (QPSK) modulation $(M = 4)$, respectively. It turns out that in almost the entire SNR region of interest, the optimal nonlinearity $F_{\min}(\rho(n))$ can be approximated without much loss in performance by $\rho(n)$ (BPSK) and $\rho(n)$ or $\rho^2(n)$ (QPSK, depending on SNR), respectively.

Experiment 2-Asymptotic Variances of Estimators (18), (11), (20), and (21) w.r.t. the UCRB: Figs. 3 and 4 depict the performance loss of the asymptotic variances (19) and (22) w.r.t.

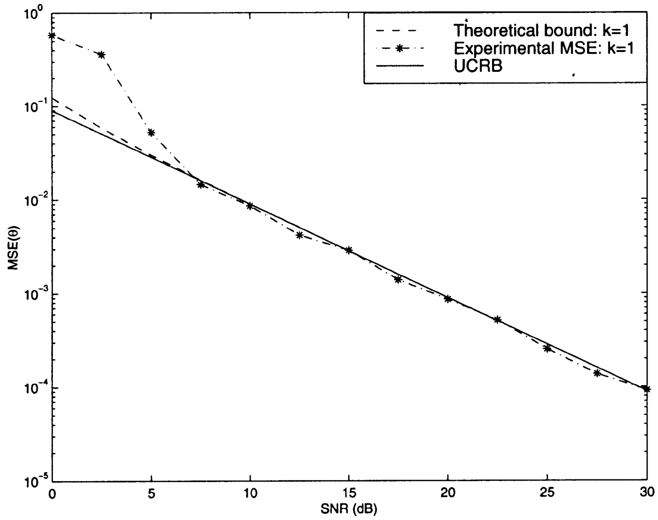

(a)

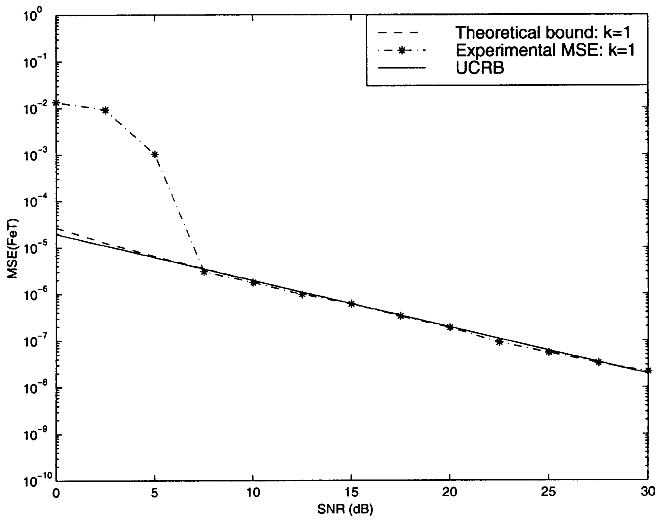

(b)

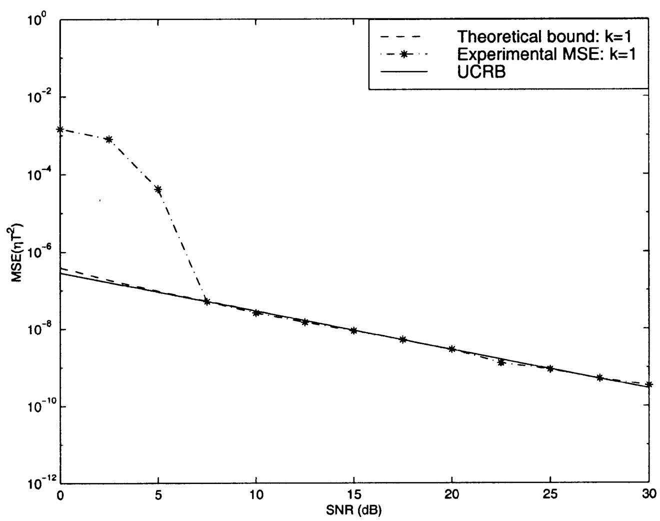

(c)

Fig. 5. (a) MSEs of $\widehat{\theta}$ versus SNR. (b) MSEs of $\widehat{F_e T}$ versus SNR. (c) MSEs of $\widehat{\eta T^2}$ versus SNR (BPSK modulation, $N = 50$).

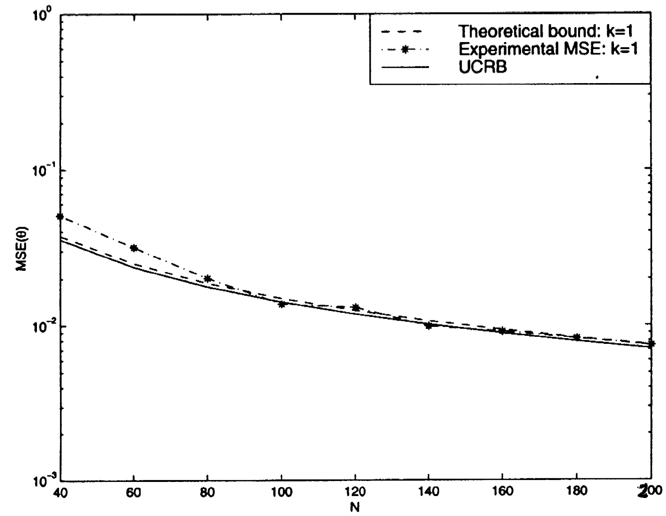

(a)

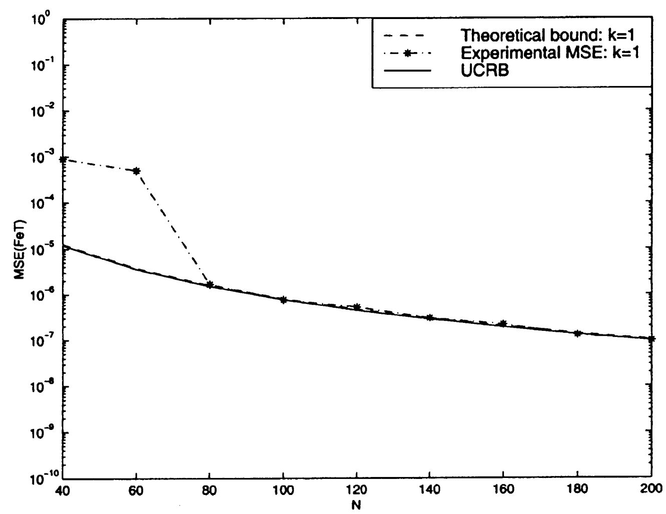

(b)

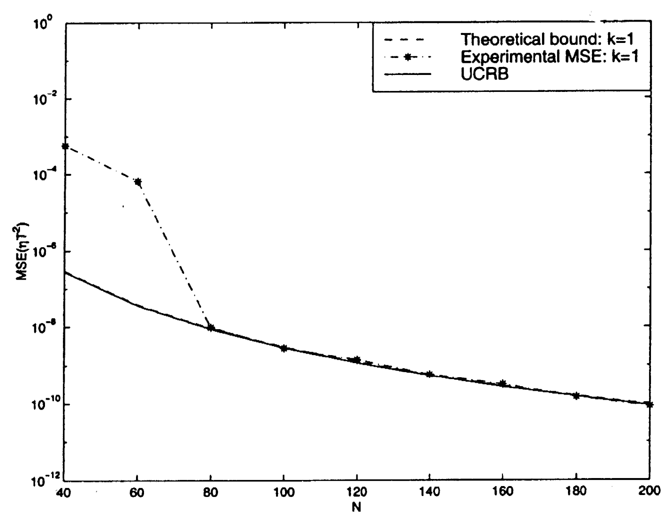

(c)

Fig. 6. (a) MSEs of $\widehat{\theta}$ versus N. (b) MSEs of $\widehat{F_e T}$ versus N. (c) MSEs of $\widehat{\eta T^2}$ versus N (BPSK modulation, SNR $= 5$ dB).

the UCRB (i.e., $-10\log_{10}[\text{avar}(\hat{\omega}_l)/\text{UCRB}(\hat{\omega}_l)]$), assuming BPSK and QPSK modulations, respectively. It can be seen that the proposed estimators exhibit good accuracy. In high SNR range they coincide with the UCRB. In low SNR range (near

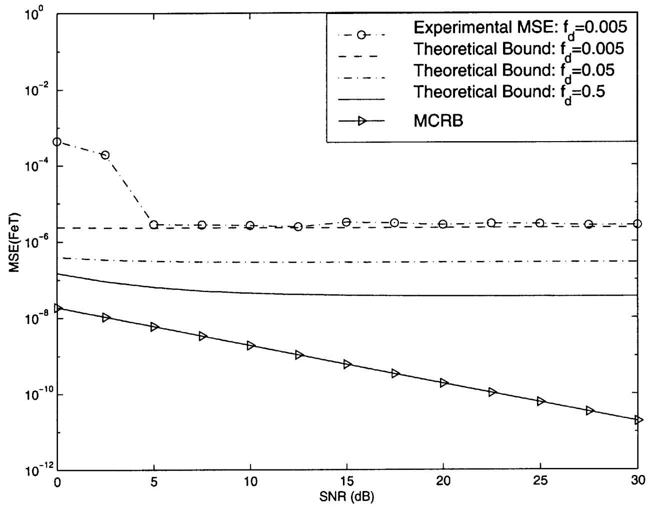

Fig. 7. MSEs of $\widehat{F_e T}$ versus SNR in the presence of a flat Ricean-fading channel (BPSK modulation).

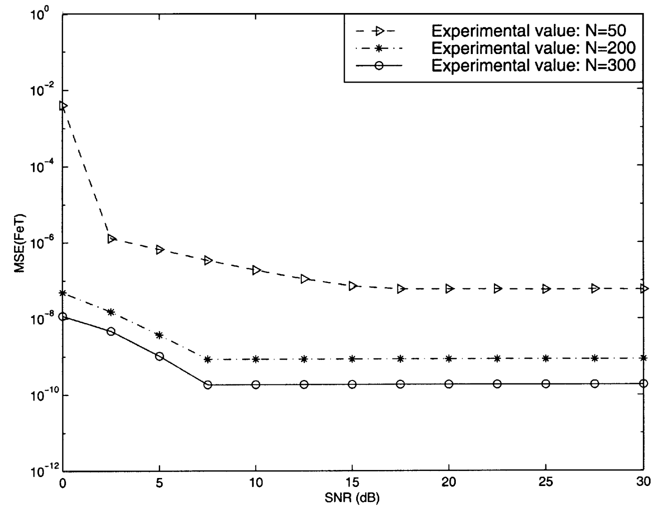

Fig. 8. MSEs of $\widehat{F_e T}$ versus SNR in the presence of timing error (BPSK modulation).

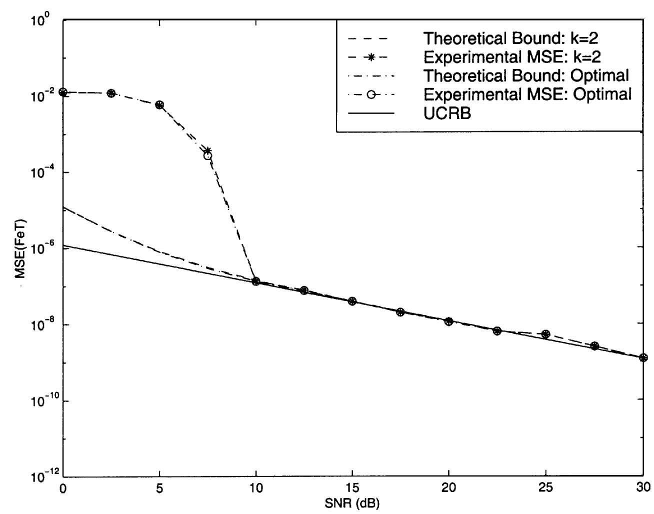

Fig. 9. MSEs of $\widehat{F_e T}$ versus SNR (QPSK modulation, $N = 50$).

0 dB), monomial nonlinear estimators with improved performance can be obtained by adopting low-order nonlinearities ($k = 1$ and 2 for BPSK and QPSK modulations, respectively). Although the matched nonlinear estimator is optimal in the entire SNR range, its performance improvement relative to the monomial estimators is observable only at low SNRs. From Figs. 1–4, we can also observe that at very high SNRs, the monomial estimators (20) and (21) for different orders k exhibit the same asymptotic variance.

Experiment 3-Comparison of the MSE of Estimators (21) With the Theoretical Bounds Versus SNR: In Fig. 5, the theoretical bounds (22) are compared with the experimental MSEs of estimators (21) versus SNR, assuming $k = 1$, $N = 50$ symbols, and BPSK modulation. This figure shows that for medium and high SNR, the experimental results are well predicted by the asymptotic bounds derived in Section IV, and the proposed estimators provide very good estimates of carrier phase, frequency offset, and Doppler rate, even when a reduced number of samples is used $(N = 50)$. This shows the potential of these estimators for fast synchronization of burst transmissions.

Experiment 4-Comparison of MSE of Estimators (21) with the Theoretical Bounds Versus Number of Samples N: Fig. 6 displays the influence of the number of samples N on the performance of the estimators (21), assuming $k = 1$, SNR $= 5$ dB, and a BPSK input modulation. One can observe from this figure that even at low SNR, the proposed NLS estimators (21) can approach very closely the UCRB using a small number of samples ($N = 70$ or 80 samples), i.e., a lower threshold of SNR, at which large estimation errors of frequency offset and Doppler rate begin to occur, can be achieved with a reduced number of samples.

Experiment 5-Performance of Frequency Estimators (29) in Flat Ricean-Fading Channels: This experiment illustrates that the proposed frequency offset estimators (29) still perform well in the presence of Ricean-fading effects. In Fig. 7, the asymptotic variance (35) and the modified CRB (MCRB) for NDA frequency offset estimation in flat Ricean-fading channel are plotted versus SNR. The latter was derived in [14], and with the notations adopted so far admits the following expression for large N : $\mathrm{MCRB}(\hat{f}_e) = 6\sigma_v^2/[4\pi^2 N^3(\rho_1^2 + \sigma_\mu^2)]$. We assume that the Ricean-fading process has a normalized energy (i.e., $\mathrm{E}\{|\mu(n)|^2\} = 1$) and the Ricean factor $\kappa := \rho_1^2/\sigma_\mu^2 = 1$. The Doppler spread f_d is chosen as 0.005, 0.05, and 0.5, respectively. The transmitted symbol is BPSK and the number of samples is chosen as $N = 200$. In Fig. 7, the MSE of estimator (29) with $k = 2$ and $f_d = 0.005$ is also plotted. From Fig. 7, it turns out that although there exists an error floor due to the random fading effects, the accuracy of the proposed frequency offset estimators is still satisfying at medium and high SNRs, and improves for large Doppler spreads.

Experiment 6-Performance of Frequency Offset Estimators (29) in the Presence of Timing Error: Until now, we assumed a perfect timing reference at receiver. The simulation results presented in Fig. 8 illustrate that estimators (29) are robust to timing errors. In this simulation, we assume that there is a normalized timing-error $\epsilon T = 0.1$, the transmit and receive filters are square-root raised cosine filters with roll-off factor $\beta = 0.5$.

The symbol modulation is BPSK, $k = 2$, and the number of samples is chosen as $N = 50$, 200, and 300, respectively.

Experiment 7-Performance of Frequency Offset Estimator With Optimal Nonlinearity: For the sake of completeness, we illustrate in Fig. 9 the performance of frequency offset estimator (29) with optimal nonlinearity (18), compared with that of $k = 2$. Both theoretical bounds are shown, too. The constellation is QPSK and the number of samples is $N = 50$. Instead of using a fixed value, this experiment considers that the true frequency offset assumes random values drawn uniformly from the interval $[-0.1, 0.1]$ during each simulation run. Fig. 9 illustrates again the merit of the performance analysis presented in this paper.

VIII. Conclusions

In this paper, we have introduced and analyzed a family of blind feedforward joint estimators for the carrier phase, frequency offset, and Doppler rate of burst-mode MPSK modulations. A matched nonlinear estimator together with a class of monomial nonlinear estimators were introduced and their performance established in closed form. It has been shown that the proposed estimators exhibit high convergence rates and good accuracy, and are robust to Ricean fading effects and timing errors. Extensions of this work to general polynomial phase signals appear straightforward.

Appendix I

Derivation of Equations (8) and (9)

Using (5), we can express $\mathrm{E}\{y(n)\}$ as follows:

$$\begin{aligned}
\mathrm{E}\{y(n)\} &= \mathrm{E}\left\{F(\rho(n))\, e^{jM\varphi(n)}\right\} \\
&= \frac{1}{M}\sum_{m=0}^{M-1}\int_0^\infty \frac{\rho(n)F(\rho(n))}{\pi\sigma_v^2} e^{-\frac{\rho^2(n)+1}{\sigma_v^2}} \int_{-\pi}^{\pi} e^{jM\varphi(n)} \\
&\quad \times e^{\frac{2\rho(n)}{\sigma_v^2}\cos\left[\varphi(n)-\frac{2\pi m}{M}-\phi(n)\right]} \mathrm{d}\varphi(n)\mathrm{d}\rho(n) \\
&= \frac{1}{M}\sum_{m=0}^{M-1} e^{j2\pi m} e^{jM\phi(n)} \\
&\quad \times \int_0^\infty \frac{2\rho(n)F(\rho(n))}{\sigma_v^2} e^{-\frac{\rho^2(n)+1}{\sigma_v^2}} \\
&\quad \times I_M\left(\frac{2\rho(n)}{\sigma_v^2}\right)\mathrm{d}\rho(n) \\
&= e^{jM\phi(n)} \int_0^\infty F(\rho(n)) \frac{I_M\left(\frac{2\rho(n)}{\sigma_v^2}\right)}{I_0\left(\frac{2\rho(n)}{\sigma_v^2}\right)} \\
&\quad \cdot \frac{2\rho(n)}{\sigma_v^2} e^{-\frac{\rho^2(n)+1}{\sigma_v^2}} I_0\left(\frac{2\rho(n)}{\sigma_v^2}\right)\mathrm{d}\rho(n) \qquad (40)
\end{aligned}$$

where in deriving the third equality we made use of the definition of $I_M(\cdot)$ [1, eq. (9.6.19)]. Then, by exploiting (6), (8) and (9) follow. Similar to (40), the following expression holds:

$$\begin{aligned}
\mathrm{E}\left\{y^2(n)\right\} &= \mathrm{E}\left\{F^2(\rho(n))\, e^{j2M\varphi(n)}\right\} \\
&= e^{j2M\phi(n)} \int_0^\infty F^2(\rho(n)) \frac{I_{2M}\left(\frac{2\rho(n)}{\sigma_v^2}\right)}{I_0\left(\frac{2\rho(n)}{\sigma_v^2}\right)} \\
&\quad \cdot \frac{2\rho(n)}{\sigma_v^2} e^{-\frac{\rho^2(n)+1}{\sigma_v^2}} I_0\left(\frac{2\rho(n)}{\sigma_v^2}\right)\mathrm{d}\rho(n)
\end{aligned}$$

which proves (16).

Appendix II

Proof of *Theorem 1*

In order to establish *Theorem 1*, let us first study the second-order statistics of additive noise $u(n)$. From (10), $u(n)$ can be expressed as

$$\begin{aligned}
u(n) &:= y(n) - \mathrm{E}\{y(n)\} \\
&= F(\rho(n))\, e^{jM\varphi(n)} - \mathrm{E}\left\{F(\rho(n))\, e^{jM\varphi(n)}\right\}.
\end{aligned}$$

Define the second-order unconjugate/conjugate autocorrelations of $u(n)$ as

$$\begin{aligned}
r_u(n;\tau) &:= \mathrm{E}\{u^*(n)u(n+\tau)\} \\
&= \mathrm{E}\left\{F(\rho(n))\, e^{-jM\varphi(n)} F(\rho(n+\tau))\, e^{jM\varphi(n+\tau)}\right\} \\
&\quad - \mathrm{E}\left\{F(\rho(n))\, e^{-jM\varphi(n)}\right\} \\
&\quad \times \mathrm{E}\left\{F(\rho(n+\tau))\, e^{jM\varphi(n+\tau)}\right\} \\
\tilde{r}_u(n;\tau) &:= \mathrm{E}\{u(n)u(n+\tau)\} \\
&= \mathrm{E}\left\{F(\rho(n))\, e^{jM\varphi(n)} F(\rho(n+\tau))\, e^{jM\varphi(n+\tau)}\right\} \\
&\quad - \mathrm{E}\left\{F(\rho(n))\, e^{jM\varphi(n)}\right\} \\
&\quad \times \mathrm{E}\left\{F(\rho(n+\tau))\, e^{jM\varphi(n+\tau)}\right\}
\end{aligned}$$

respectively. Due to (7), it turns out that $r_u(n;\tau)$ and $\tilde{r}_u(n;\tau)$ are both equal to zero if $\tau \neq 0$. Hence, we obtain from (9), (15), and (16) the following relations:

$$\begin{aligned}
r_u(n;\tau) &= \left[\mathrm{E}\left\{F^2(\rho(n))\right\} - \left|\mathrm{E}\left\{F(\rho(n))\, e^{jM\varphi(n)}\right\}\right|^2\right]\delta(\tau) \\
&= (\mathcal{B} - \mathcal{C}^2)\delta(\tau) \qquad (41) \\
\tilde{r}_u(n;\tau) &= \left[\mathrm{E}\left\{F^2(\rho(n))\, e^{j2M\varphi(n)}\right\}\right. \\
&\quad \left. - \mathrm{E}^2\left\{F(\rho(n))\, e^{jM\varphi(n)}\right\}\right]\delta(\tau) \\
&= (\mathcal{D} - \mathcal{C}^2) e^{j2M\phi(n)}\delta(\tau) \qquad (42)
\end{aligned}$$

where $\delta(.)$ stands for Kronecker's delta.

Next, we begin the derivation of *Theorem 1*. Considering the Taylor series expansion of $\hat{\mathcal{C}}\exp(j\sum_{l=0}^{2}\hat{\omega}_l n^l)$ in the neighborhood of the true value $[\mathcal{C}\;\;\omega_0\;\;\omega_1\;\;\omega_2]^T$, we can write

$$\begin{aligned}
\hat{\mathcal{C}} e^{j\sum_{l=0}^{2}\hat{\omega}_l n^l} &= \mathcal{C} e^{j\sum_{l=0}^{2}\omega_l n^l} + (\hat{\mathcal{C}} - \mathcal{C}) e^{j\sum_{l=0}^{2}\omega_l n^l} \\
&\quad + j\sum_{k=0}^{2} n^k(\hat{\omega}_k - \omega_k)\mathcal{C} e^{j\sum_{l=0}^{2}\omega_l n^l} + \mathrm{rem}
\end{aligned}$$

where rem stands for the high-order remainder terms which asymptotically as $N \to \infty$ can be neglected. Thus, we can approximate (12) by

$$J(\hat{\boldsymbol{\omega}}) \doteq \frac{1}{2}\sum_{n=0}^{N-1}\left|y(n) - \mathcal{C}e^{j\sum_{l=0}^{2}\omega_l n^l} - (\hat{\mathcal{C}} - \mathcal{C})e^{j\sum_{l=0}^{2}\omega_l n^l} - j\sum_{k=0}^{2} n^k(\hat{\omega}_k - \omega_k)\mathcal{C}e^{j\sum_{l=0}^{2}\omega_l n^l}\right|^2.$$

Setting the derivatives of $J(\hat{\boldsymbol{\omega}})$ w.r.t. $\hat{\boldsymbol{\omega}}$ to 0, we obtain[2]

$$\sum_{n=0}^{N-1}\Re\left\{u(n)e^{-jM\phi(n)}\right\} - N(\hat{\mathcal{C}} - \mathcal{C}) = 0$$

$$\sum_{n=0}^{N-1} n^k \Im\left\{u(n)e^{-jM\phi(n)}\right\} - \mathcal{C}\sum_{l=0}^{2}(\hat{\omega}_l - \omega_l)\sum_{n=0}^{N-1} n^{k+l} = 0, \qquad k = 0, 1, 2.$$

We normalize the above equations by $N^{1/2}$ and $N^{k+1/2}$, $k =$ 0, 1, 2, respectively, and obtain that asymptotically $(N \to \infty)$ the following relations hold (c.f. [13]):

$$\frac{1}{\sqrt{N}}\sum_{n=0}^{N-1}\Re\left\{u(n)e^{-jM\phi(n)}\right\} = \sqrt{N}(\hat{\mathcal{C}} - \mathcal{C}) \tag{43}$$

$$\begin{aligned}\frac{1}{\sqrt{N}}\sum_{n=0}^{N-1}\left(\frac{n}{N}\right)^k \Im\left\{u(n)e^{-jM\phi(n)}\right\} &= \mathcal{C}\sum_{l=0}^{2} N^{\frac{l+1}{2}}(\hat{\omega}_l - \omega_l)\left(\frac{1}{N}\sum_{n=0}^{N-1}\left(\frac{n}{N}\right)^{k+l}\right)\\ &= \sum_{l=0}^{2}\frac{\mathcal{C}}{k+l+1}N^{l+\frac{1}{2}}(\hat{\omega}_l - \omega_l), \quad k = 0, 1, 2\end{aligned} \tag{44}$$

where in deriving the last equality, we made use of the well-known limit [16]

$$\lim_{N\to\infty}\frac{1}{N}\sum_{n=0}^{N-1}\left(\frac{n}{N}\right)^k = \frac{1}{k+1}.$$

Next, we express (43) and (44) in the matrix compact form equation

$$\mathbf{K_N}(\hat{\boldsymbol{\omega}} - \boldsymbol{\omega}) = \boldsymbol{\Lambda}^{-1}\boldsymbol{\varepsilon} \tag{45}$$

$$\mathbf{K_N} := \begin{bmatrix} N^{\frac{1}{2}} & 0 & 0 & 0\\ 0 & N^{\frac{1}{2}} & 0 & 0\\ 0 & 0 & N^{\frac{3}{2}} & 0\\ 0 & 0 & 0 & N^{\frac{5}{2}}\end{bmatrix}$$

$$\boldsymbol{\Lambda} := \begin{bmatrix} 1 & 0 & 0 & 0\\ 0 & \mathcal{C} & \frac{\mathcal{C}}{2} & \frac{\mathcal{C}}{3}\\ 0 & \frac{\mathcal{C}}{2} & \frac{\mathcal{C}}{3} & \frac{\mathcal{C}}{4}\\ 0 & \frac{\mathcal{C}}{3} & \frac{\mathcal{C}}{4} & \frac{\mathcal{C}}{5}\end{bmatrix}$$

$$\boldsymbol{\varepsilon} := \begin{bmatrix} \frac{1}{\sqrt{N}}\sum_{n=0}^{N-1}\Re\left\{u(n)e^{-jM\phi(n)}\right\}\\ \frac{1}{\sqrt{N}}\sum_{n=0}^{N-1}\Im\left\{u(n)e^{-jM\phi(n)}\right\}\\ \frac{1}{\sqrt{N}}\sum_{n=0}^{N-1}\left(\frac{n}{N}\right)\Im\left\{u(n)e^{-jM\phi(n)}\right\}\\ \frac{1}{\sqrt{N}}\sum_{n=0}^{N-1}\left(\frac{n}{N}\right)^2\Im\left\{u(n)e^{-jM\phi(n)}\right\}\end{bmatrix}. \tag{46}$$

Since in (45) only $\boldsymbol{\varepsilon}$ is random, the asymptotic covariance matrix of $\hat{\boldsymbol{\omega}}$ can be expressed as

$$\begin{aligned}\boldsymbol{\Sigma}_{\hat{\boldsymbol{\omega}}} &:= \lim_{N\to\infty}\mathrm{E}\left\{\mathbf{K_N}(\hat{\boldsymbol{\omega}} - \boldsymbol{\omega})(\hat{\boldsymbol{\omega}} - \boldsymbol{\omega})^T\mathbf{K_N}^T\right\}\\ &= \lim_{N\to\infty}\mathrm{E}\left\{\boldsymbol{\Lambda}^{-1}\boldsymbol{\varepsilon}\boldsymbol{\varepsilon}^T\boldsymbol{\Lambda}^{-1}\right\}\\ &= \boldsymbol{\Lambda}^{-1}\mathbf{R}_{\boldsymbol{\varepsilon}}\boldsymbol{\Lambda}^{-1}\end{aligned} \tag{47}$$

where $\mathbf{R}_{\hat{\boldsymbol{\varepsilon}}} := \lim_{N\to\infty}\mathrm{E}\{\boldsymbol{\varepsilon}\boldsymbol{\varepsilon}^T\}$.

Observe that

$$\begin{aligned}\mathbf{R}_{\boldsymbol{\varepsilon}}(1,1) &= \lim_{N\to\infty}\frac{1}{N}\mathrm{E}\left[\left(\sum_{n=0}^{N-1}\Re\left\{u(n)e^{-jM\phi(n)}\right\}\right)^2\right]\\ &= \lim_{N\to\infty}\frac{1}{4N}\sum_{n_1,n_2=0}^{N-1}\\ &\quad\times\mathrm{E}\left\{\left[u(n_1)e^{-jM\phi(n_1)} + u^*(n_1)e^{jM\phi(n_1)}\right]\right.\\ &\quad\times\left.\left[u(n_2)e^{-jM\phi(n_2)} + u^*(n_2)e^{jM\phi(n_2)}\right]\right\}.\end{aligned}$$

Using (41) and (42), $\mathbf{R}_{\boldsymbol{\varepsilon}}(1,1)$ can be written as

$$\mathbf{R}_{\boldsymbol{\varepsilon}}(1,1) = \lim_{N\to\infty}\frac{1}{2N}\sum_{n=0}^{N-1}(\mathcal{D}+\mathcal{B}-2\mathcal{C}^2) = \frac{1}{2}(\mathcal{D}+\mathcal{B}-2\mathcal{C}^2).$$

Similarly, we obtain $\mathbf{R}_{\boldsymbol{\varepsilon}}(1,k) = 0$, $k = 2, 3, 4$, which means that the NLS estimators of the amplitude and phase parameters are asymptotically decoupled.

To evaluate the asymptotic variance of $\hat{\omega}_l$, $l = 0, 1, 2$, we need to compute for k, $m = 0, 1, 2$

$$\begin{aligned}\mathbf{R}_{\boldsymbol{\varepsilon}}(2+k, 2+m) &= \lim_{N\to\infty}\frac{1}{N}\sum_{n_1,n_2=0}^{N-1}\left(\frac{n_1}{N}\right)^k\left(\frac{n_2}{N}\right)^m\\ &\quad\times\mathrm{E}\left[\Im\left\{u(n_1)e^{-jM\phi(n_1)}\right\}\Im\left\{u(n_2)e^{-jM\phi(n_2)}\right\}\right].\end{aligned}$$

Using the same technique as for $\mathbf{R}_{\boldsymbol{\varepsilon}}(1,1)$, we obtain

$$\mathbf{R}_{\boldsymbol{\varepsilon}}(2+k, 2+m) = \frac{1}{2(k+m+1)}(\mathcal{B}-\mathcal{D}), \qquad k, m = 0, 1, 2.$$

Thus, the matrix $\mathbf{R}_{\boldsymbol{\varepsilon}}$ can be expressed as

$$\mathbf{R}_{\boldsymbol{\varepsilon}} = \frac{1}{2}\begin{bmatrix}\mathcal{B}+\mathcal{D}-2\mathcal{C}^2 & 0\\ 0 & (\mathcal{B}-\mathcal{D})\mathbf{H}\end{bmatrix} \tag{48}$$

where $\mathbf{H} := \{1/(k+l+1)\}_{k,l=0}^{2}$ is the so-called Hilbert matrix [20]. Note that

$$\boldsymbol{\Lambda}^{-1} = \begin{bmatrix}1 & 0\\ 0 & \mathcal{C}^{-1}\mathbf{H}^{-1}\end{bmatrix}.$$

Therefore, the asymptotic covariance matrix of $\hat{\boldsymbol{\omega}}$ is obtained as

$$\begin{aligned}\boldsymbol{\Sigma}_{\hat{\boldsymbol{\omega}}} &= \boldsymbol{\Lambda}^{-1}\mathbf{R}_{\boldsymbol{\varepsilon}}\boldsymbol{\Lambda}^{-1}\\ &= \frac{1}{2}\begin{bmatrix}\mathcal{B}+\mathcal{D}-2\mathcal{C}^2 & 0\\ 0 & (\mathcal{B}-\mathcal{D})\mathcal{C}^{-2}\mathbf{H}^{-1}\end{bmatrix}\end{aligned} \tag{49}$$

[2]The notations $\Re$ and $\Im$ stand for the real and imaginary part of a complex-valued number, respectively.

where the inverse of the Hilbert matrix $\mathbf{H}$ is given by [20]

$$\mathbf{H}^{-1}(k,l) = (-1)^{k+l}\frac{(k+3)!(l+3)!}{(k!)^2(l!)^2(2-k)!(2-l)!(k+l+1)}. \quad (50)$$

Based on (49) and (50), some direct computations lead to the sought asymptotic variances (14). This concludes the proof of *Theorem 1*.

REFERENCES

[1] *Handbook of Mathematical Functions*, M. Abramowitz and I. A. Stegun, Eds., National Bureau of Standards, Washington, DC, 1964.

[2] S. Bellini, C. Molinari, and G. Tartara, "Digital frequency estimation in burst mode QPSK transmission," *IEEE Trans. Commun.*, vol. 38, pp. 959–961, July 1990.

[3] S. Bellini, "Frequency estimators for MPSK operating at one sample per symbol," in *Conf. Rec. GLOBECOM'94*, San Francisco, CA, 1994, pp. 962–966.

[4] C. Bergogne, P. Sehier, and M. Bousquet, "Reduced complexity frequency estimator for burst transmission," in *Conf. Rec. GLOBECOM'95*, vol. 2, 1995, pp. 1318–1322.

[5] ——, "Reduced complexity frequency estimator applied to burst transmission," in *Proc. 4th IEEE Int. Conf. Universal Personal Communications*, 1995, pp. 231–235.

[6] O. Besson, M. Ghogho, and A. Swami, "Parameter estimation for random amplitude chirp signals," *IEEE Trans. Signal Processing*, vol. 47, pp. 3208–3219, Dec. 1999.

[7] J. C.-I. Chuang and N. R. Sollenberger, "Burst coherent demodulation with combined symbol timing, frequency offset estimation, and diversity selection," *IEEE Trans. Commun.*, vol. 39, pp. 1157–1164, July 1991.

[8] F. Classen, H. Meyr, and P. Sehier, "Maximum likelihood open loop carrier synchronizer for digital radio," in *Conf. Rec. ICC'93*, Geneva, Switzerland, 1993, pp. 493–497.

[9] S. N. Crozier, "Low complexity frequency estimator with close-to-optimum performance," in *Conf. Rec. PIRM'93*, vol. 1, 1993, pp. 426–430.

[10] M. P. Fitz, "Nonlinear digital carrier synchronization for Rician fading channels," in *Conf. Rec. GLOBECOM'90*, San Diego, CA, 1990, pp. 623–628.

[11] J. M. Francos and B. Friedlander, "Bounds for estimation of multicomponent signals with random amplitude and deterministic phase," *IEEE Trans. Signal Processing*, vol. 43, pp. 1161–1172, May 1995.

[12] M. Ghogho, A. K. Nandi, and A. Swami, "Cramèr–Rao bounds and maximum-likelihood estimation for random amplitude phase-modulated signals," *IEEE Trans. Signal Processing*, vol. 47, pp. 2905–2916, Nov. 1999.

[13] M. Ghogho and A. Swami, "Non-efficiency of the nonlinear least-squares estimator of polynomial phase signals in colored noise," in *Conf. Rec. Asilomar'98*, Pacific Grove, CA, 1998, pp. 1447–1451.

[14] F. Gini and R. Reggiannini, "On the use of Cramér–Rao-like bounds in the presence of random nuisance parameters," *IEEE Trans. Commun.*, vol. 48, pp. 2120–2126, Dec. 2000.

[15] I. S. Gradshteyn and I. M. Ryzhik, *Table of Integrals, Series, and Products*. New York: Academic, 1965.

[16] T. Hasan, "Nonlinear time series regression for a class of amplitude modulated cosinusoids," *J. Time Series Anal.*, vol. 3, no. 2, pp. 109–122, 1982.

[17] G. D. Jonghe and M. Moeneclaey, "Optimal averaging filter length of the Viterbi and Viterbi carrier synchronizer for a given frequency offset," in *Conf. Rec. GLOBECOM'94*, San Francisco, CA, 1994, pp. 1363–1368.

[18] F. Mazzenga and G. E. Corazza, "Blind least-squares estimation of carrier phase, Doppler shift, and Doppler rate for MPSK burst transmission," *IEEE Commun. Lett.*, vol. 2, pp. 73–75, Mar. 1998.

[19] U. Mengali and A. N. D'Andrea, *Synchronization Techniques for Digital Receivers*. New York: Plenum, 1997.

[20] K. S. Miller, *Some Eclectic Matrix Theory*. Malabar, FL: Krieger, 1987.

[21] B. E. Paden, "A matched nonlinearity for phase estimation of a PSK-modulated carrier," *IEEE Trans. Inform. Theory*, vol. IT-32, pp. 419–422, May 1986.

[22] D. R. Pauluzzi and N. C. Beaulieu, "A comparison of SNR estimation techniques for the AWGN channel," *IEEE Trans. Commun.*, vol. 48, pp. 1681–1691, Oct. 2000.

[23] J. P. Seymour and M. P. Fitz, "Nonlinear digital phase estimation for mobile communications," in *Conf. Rec. PIMRC'92*, Boston, MA, 1992, pp. 194–198.

[24] P. Stoica and R. Moses, *Introduction to Spectral Analysis*. Englewood Cliffs, NJ: Prentice-Hall, 1997.

[25] A. J. Viterbi and A. M. Viterbi, "Nonlinear estimation of PSK-modulated carrier phase with application to burst digital transmissions," *IEEE Trans. Inform. Theory*, vol. IT-29, pp. 543–551, July 1983.

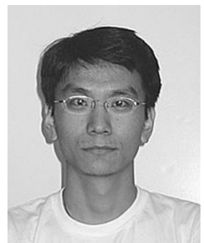

Yan Wang received the B.S. degree from the Department of Electronics, Peking University, Beijing, China, in 1996 and the M.Sc. degree from the School of Telecommunications Engineering, Beijing University of Posts and Telecommunications (BUPT), in 1999.

From 1999 to 2000, he was a member of BUPT-Nortel R&D Center, Beijing. Since 2000, he has been a Research Assistant with the Department of Electrical Engineering, Texas A&M University, College Station. His research interests are in the area of statistical signal processing and its applications in wireless communication systems.

Erchin Serpedin received (with highest distinction) the Diploma of electrical engineering form the Polytechnic Institute of Bucharest, Bucharest, Romania, in 1991. He received the specialization degree in signal processing and transmission of information from Ecole Superiéure D'Electricité, Paris, France, in 1992, the M.Sc. degree from Georgia Institute of Technology, Atlanta, in 1992, and the Ph.D. degree from the University of Virginia, Charlottesville, in 1998.

From 1993 to 1995, he was an instructor with the Polytechnic Institute of Bucharest, and between January and June 1999, he was a Lecturer with the University of Virginia. In July 1999, he joined the Wireless Communication Laboratory, Texas A&M University, College Station, as an Assistant Professor. His research interests lie in the areas of statistical signal processing and wireless communications.

Dr. Serpedin received the NSF Career Award in 2001. He is currently an Associate Editor for the IEEE COMMUNICATIONS LETTERS and the IEEE SIGNAL PROCESSING LETTERS.

Philippe Ciblat was born in Paris, France, in 1973. He received the Engineer degree from Ecole Nationale Supérieure des Télécommunications (ENST), Paris, the M.Sc. in signal processing from University of Paris-Sud, Orsay, France, in 1996, and the Ph.D. degree from the University of Marne-la-Vallée, Noisy le Grand, France, in July 2000.

From October 2000 to June 2001, he was a Postdoctoral Researcher with the Communications and Remote Sensing Department, Université Catholique de Louvain, Louvain-la-Neuve, Belgium. He is currently an Associate Professor with the Department of Communications and Electronics, ENST. His research areas include statistical and digital signal processing, especially blind equalization and synchronization.